ARTICLES

Journal of Semiconductors
(2019) 40, 022403
doi: 10.1088/1674-4926/40/2/022403

Mobility impact on compensation performance of AMOLED pixel circuit using IGZO TFTs

Congwei Liao†

Shenzhen Graduate School, Peking University, Shenzhen 518055, China

Abstract: The suitability of indium gallium zinc oxide (IGZO) thin-film transistors (TFT) for implementation of active matrix display of organic light emitting diodes (AMOLED) compensation pixel circuits is addressed in this paper. In particular, the impact of mobility on compensating performance for the implementation in AMOLED pixel circuits is investigated. Details of the effective mobility modeling using the power law of gate-to-source voltage are provided, and parameters are extracted according to the measured current-to-voltage data of IGZO TFT samples. The investigated AMOLED pixel circuit consists of 4 switching TFTs, 1 driving TFT, and 1 capacitor. A "source-follower" structure is used for the threshold voltage extraction of the driving transistor. A new timing diagram is proposed; thus the current error of the pixel circuit is almost independent of the effective mobility. But, to improve the precision of the threshold voltage extraction of the driving transistor, the mobility is required to be greater than 5 $cm^2V^{-1}s^{-1}$. On the other hand, the optimized storage capacitance is reversely proportional to the effective mobility. Thus, the layout area of the pixel circuit can be decreased from 100×100 to 100×68 μm^2, with the effective mobility increased from 10 to 50 $cm^2V^{-1}s^{-1}$. Therefore, IGZO TFT is a good alternative backplane technology for AMOLED displays, and a higher effective mobility is preferred for high compensation performance and compact layout.

Key words: IGZO TFT; pixel circuit; mobility

Citation: C W Liao, Mobility impact on compensation performance of AMOLED pixel circuit using IGZO TFTs[J]. *J. Semicond.*, 2019, 40(2), 022403. http://doi.org/10.1088/1674-4926/40/2/022403

1. Introduction

Due to the rapid development in recent years, indium gallium zinc oxide (IGZO) thin film transistors (TFTs) are expected to be the dominant technology for the next generation of flat panel display[1]. Owing to the merits of high mobility, decent reliability, and excellent uniformity, IGZO TFTs are suitable for pixel-circuits, driving-circuits, and sensing-circuits on display panels[2–5]. Previously, much research focused on using IGZO TFTs for liquid crystalline display (LCD) and active matrix display of organic light emitting diodes display (AMOLED) with large dimensions. It is well known that, AMOLED for mobile displays are dominantly implemented by low temperature poly-crystalline silicon TFTs (LTPS TFTs) at present, and maybe by low temperature poly-crystalline silicon and oxide TFTs (LTPO) for the near future[6]. Whether AMOLED for mobile displays could be completely implemented with IGZO TFTs is still an open question. Compared with LTPS TFTs, the main drawback of IGZO TFTs is the lower mobility. As the requirement of driving ability and stability of the driving transistor is much higher than that of switching transistors, it might be concluded that the mobility of IGZO TFTs isn't sufficient for mobile AMOLED display panels[7, 8]. In addition, IGZO TFTs are also prone to performance degradation after long operating times, which leads to complicated pixel circuit topology to compensate for TFT's degradations. On the other hand, the advantage of the IGZO TFTs is the decreased cost over the large manufacturing area compared to that of the LTPS TFTs. Therefore, it is beneficial to the mass production of AMOLED if new driving methods for IGZO TFTs integrated pixels can be found.

In the past years, many new processes and materials for high performance metal oxide TFTs were proposed. It seems that high mobility TFTs can be obtained even with IGZO as the active layer, owning to novel device structures, such as dual-gate[9], vertical channel[10], and dual-active layer[11]. But more recently, there have been few discussions on the impact of mobility on performances of AMOLED display with IGZO TFTs. Nathan *et al.* previously demonstrated the influence of mobility on the resolution of AMOLED with amorphous silicon TFTs, which have a typical mobility of 0.3 $cm^2V^{-1}s^{-1}$[12]. It was interesting that even amorphous silicon TFTs are capable of implementing AMOLED display, and it seems that the mobility isn't a limiting factor for the shrinking of pixel size. However, the demonstrated pixel circuit is on the basis of current programming, which requires long settling time and it isn't practical for high resolution displays. In contrast to Nathan's conclusions, Jang *et al.* recently demonstrated that the compensating efficiency is strongly dependent on the device mobility[13]. It was demonstrated that, for accurate threshold-voltage-extraction, the mobility is required to be higher than 30 $cm^2V^{-1}s^{-1}$, otherwise a large current error is caused by the threshold voltage shift of the driving transistor. Therefore, it is of great interest to see how the mobility impact the implementation of AMOLED display?

In this paper, the impact of mobility on the performances of AMOLED pixel circuit with IGZO TFTs is investigated. The effective mobility and current-to-voltage characteristics are

Correspondence to: C W Liao, HUSTLIAO@126.com
Received 16 OCTOBER 2017; Revised 15 NOVEMBER 2018.

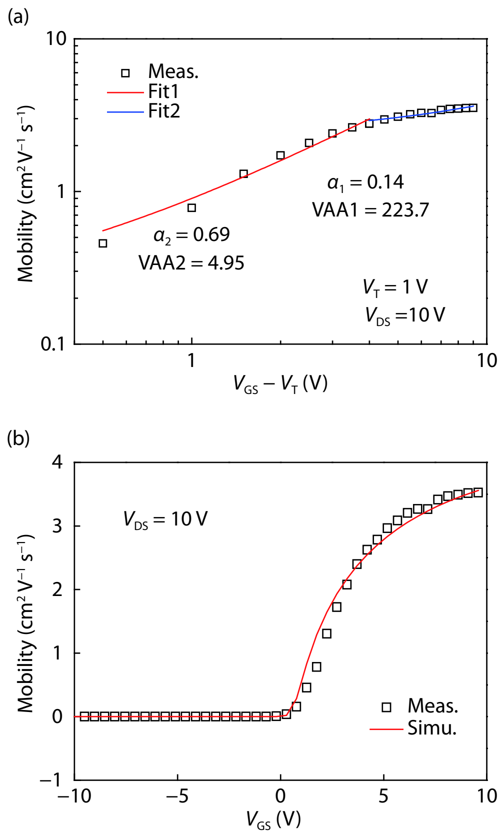

Fig. 1. (Color online) (a) The fitting curve of the extracted measured mobility and (b) comparison of the measured and the simulated mobility for IGZO TFTs.

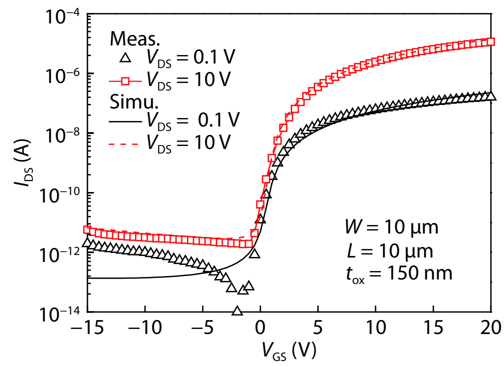

Fig. 2. (Color online) The current-to-voltage curve of IGZO TFT with measured and simulated results.

modeled and compared with the measured results. Then a typical AMOLED pixel circuit with IGZO TFTs is taken as an example to investigate the impact of IGZO TFT's mobility on the compensation rate. In additions, the relationship between the mobility and pixel layout area is discussed.

2. Modeling of mobility and current-to-voltage characteristics

Prior to discussion of the mobility impact on the AMOLED pixel performance, firstly the modeling of IGZO TFT's mobility is carried out. Here, the RPI model with LEVEL = 35 is used. The fabricated IGZO TFT samples are with the conventional back channel etched structure and the electrical performance is measured using Keithley 4200 with room temperature. The channel length and width of the measured TFT is 10 and 10 μm, respectively. The insulating layer is SiO_x with a thickness of 150 nm.

The modeling of mobility is a critical process for parameter extractions of RPI model. It is worth noting here that being different from crystalline semiconductor transistors, the mobility of amorphous transistors follow a power law of the voltage[14, 15], which is expressed as

$$\mu_{FE} = \mu_0 \left(\frac{V_{GS} - V_T}{V_{AA}} \right)^{\alpha}. \quad (1)$$

Here μ_0 is the band mobility, V_{AA} is the characteristic voltage, V_T is the threshold voltage, and α is the power law coefficient. Then, the effective mobility can be extracted through the measured current-to-voltage data[16–19].

It is known that the relationship of drain-to-source current to gate-to-source voltage for the saturation regions ($V_{DS} \geqslant V_{GS} - V_T$), can be modeled as

$$I_{DS} = \mu_{FE} C_I \frac{W}{2L} (V_{GS} - V_T)^2, \quad (2)$$

where C_I is the insulating capacitance per unit area, W and L are the width and length of IGZO channel, respectively. While for the linear region ($V_{DS} < V_{GS} - V_T$), the current-to-voltage relationship is modeled by

$$I_{DS} = \mu_{FE} C_I \frac{W}{L} (V_{GS} - V_T) V_{DS}. \quad (3)$$

For AMOLED pixels, the driving transistor is the most important element, as it converts the input data voltage to the driving current of OLED pixels. For reliable operations, the driving transistor is biased in the saturation region to prevent the voltage drop on power source lines, i.e. V_{DD}. Therefore, we use the measured data in the saturation region for mobility extraction and modeling. By differentiating two adjacent current and voltage, the effective mobility can be calculated as

$$\mu_{FE} = \frac{2L}{WC_I} \left(\frac{\sqrt{I_{DS2}} - \sqrt{I_{DS1}}}{V_{GS2} - V_{GS1}} \right)^2. \quad (4)$$

Then by rearranging Eq. (1), it can be derived that

$$\log(\mu_{FE}) = \alpha [\log(V_{GS} - V_T) - \log(V_{AA})] + \log(\mu_0). \quad (5)$$

Theoretically speaking, then by fitting the $\log(\mu_{FE})$ to $\log(V_{GS} - V_T)$ curve, the mobility related parameters can be derived.

Fig. 1 shows the fitting curve of the extracted measured mobility (a), and the comparison of the measured and the simulated mobility (b) for IGZO TFTs. Actually, the fitting curve for $\log(\mu_{FE})$ to $\log(V_{GS} - V_T)$ isn't continuous for the different operating regimes. Thus, besides the parameters shown in Eq. (5) (i.e. α, V_{AA}, μ_0), there are other shape related parameters for the accurate mobility modeling using RPI model (LEVEL 35)[20]. In other words, the fitting method shown above only provides an initial guess for determining the RPI parameters. After several iterations, parameters of the effective mobility can be determined. The parameters of RPI model related with effective mobility are listed in Table 1. It can be seen that decent agreement can be obtained between the measured and the simulated effect-

Table 1. Values of parameters in the RPI model related to effective mobility.

Parameter	Value
MUBAND ($m^2V^{-1}s^{-1}$)	2.11
GAMMA	0.95
V_{AA} (V)	45 550
V_{MIN} (V)	0.02
DELTA	24
ALPHASAT	1.0
V_{T0} (V)	0.5
V_{FB} (V)	−2.2

ive mobility. However, in the case that V_{GS} approximates V_T, there is observed discrepancy between the measured and simulation results. This is because, for the sub-threshold region, the current-to-voltage relationship cannot be expressed as Eq. (2) or Eq. (3), thus the extracted effective mobility is not accurate enough. The overall measured mobility–voltage characteristics could well be reproduced by the RPI model. Therefore, in the following part, the extracted mobility model is used to analyze the influence of mobility on the performance of AMOLD pixel circuits.

On the basis of the extracted mobility, by further tuning the physical parameters according to the TFT process, and properly adjusting the fitting parameters in the RPI models, excellent fitting can be obtained between the simulation and calculation results of drain-to-source current versus the gate-to-source voltage as shown in Fig. 2. However, due to the complicated leakage current path, there is still discrepancy in the backward leakage region. For practical AMOLED pixel operation, the IGZO TFTs mainly operate in the above-threshold and the near-threshold voltage regions, thus it is sufficiently accurate for the SPICE studies.

3. Results and discussions

3.1. Pixel circuit descriptions

The investigated pixel schematic and the timing diagram are shown in Fig. 3. Being different from the previous timing diagram shown by Kawashima *et al.*[3], the presented timing diagram here is new. It is worth noting that, there is an overlap period between V_{SCAN} and V_{EM2} for the initialization procedure (1). This is important for clearing the remaining charges of C_S. For this overlap period the left and right electrodes of C_S are charged with V_{DATA} and V_{OLED} + E_{VSS}, respectively. Thus, the source electrode of the driving transistor, i.e. the right electrode of C_S is discharged to a lower voltage to initialize the 'source follower' structure.

On the other hand, there is no overlap between the V_{SCAN} and V_{EM2} for the previous schematics. Then, the initializations for the left and right electrodes of C_S take place for different time intervals. Although being pre-charged with V_{OLED} + E_{VSS} through the turned-on T_{EM}, the source electrode of the driving transistor is prone to be disturbed by the following data input due to the voltage coupling effect of C_S. In this case, the precision of V_T extraction through the 'source follower' structure is reversely influenced. Thus, compared with the previous schematic, the proposed driving method has better programming and V_T compensating ability.

The operating procedures of the investigated pixel circuit are divided into (1) initialization, (2) data input, and (3) light emitting, as shown in Fig. 3(b). The operating details are described as follows.

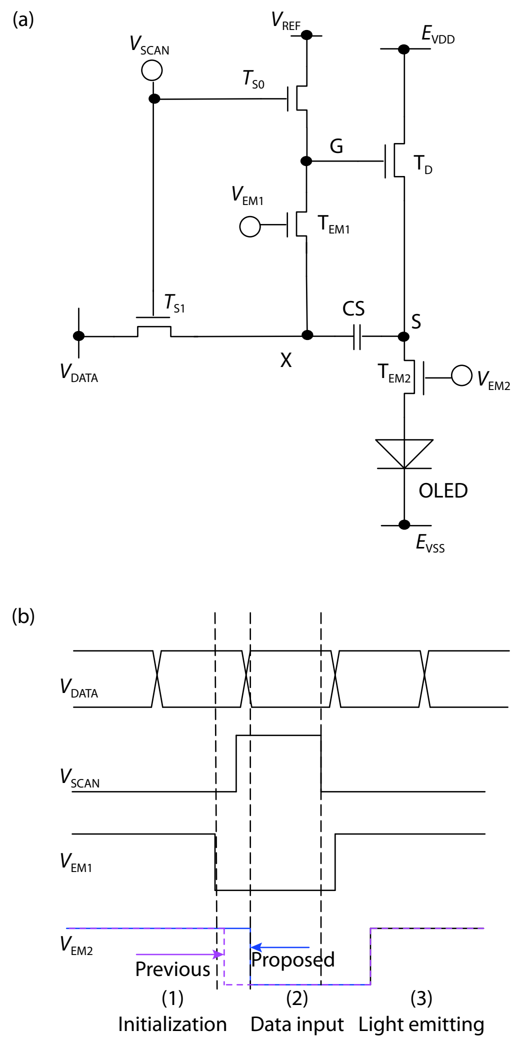

Fig. 3. (Color online) (a) IGZO TFT integrated AMOLED pixel circuit and (b) the timing diagram.

(1) Initialization

For this period, the voltage of V_{EM2} and V_{SCAN} are high, and the level of V_{EM1} is low. Then, the switching transistors, i.e. T_{S0}, T_{S1} and T_{EM2} are turned on. Consequently, the left and right electrodes of C_S are charged with V_{DATA} and V_{OLED} + E_{VSS}, respectively. The internal node G, i.e. the gate electrode of the driving transistor t_D is charged with V_{REF} through T_{S0}.

(2) Data input

Then, the level of scan signal V_{SCAN} is high, and the emit-controlling signals V_{EM1} and V_{EM2} are switched to low. Thus, the switching transistor T_{EM2} is turned off. Consequently, the source electrode of the driving transistor, i.e. the right terminal of the storage capacitance C_S, is charged with $V_{REF} - V_T$. On the other hand, the data voltage is transferred to the left terminal of the storage capacitance C_S. Thus, the voltage difference of ($V_{DATA} - V_{REF} + V_T$) is programmed and stored by C_S. In other words, the threshold voltage information of the driving transistor is stored by C_S. This is a typical 'source follower' structure, and the analysis in this paper can also be applied to lots of other similar circuits.

(3) Light emitting

For the light emitting period, both the voltage of V_{EM1} and V_{EM2} are turned to high, and the voltage of the scan signal V_{SCAN} is low. Thus, the stored charges in the capacitance C_S are al-

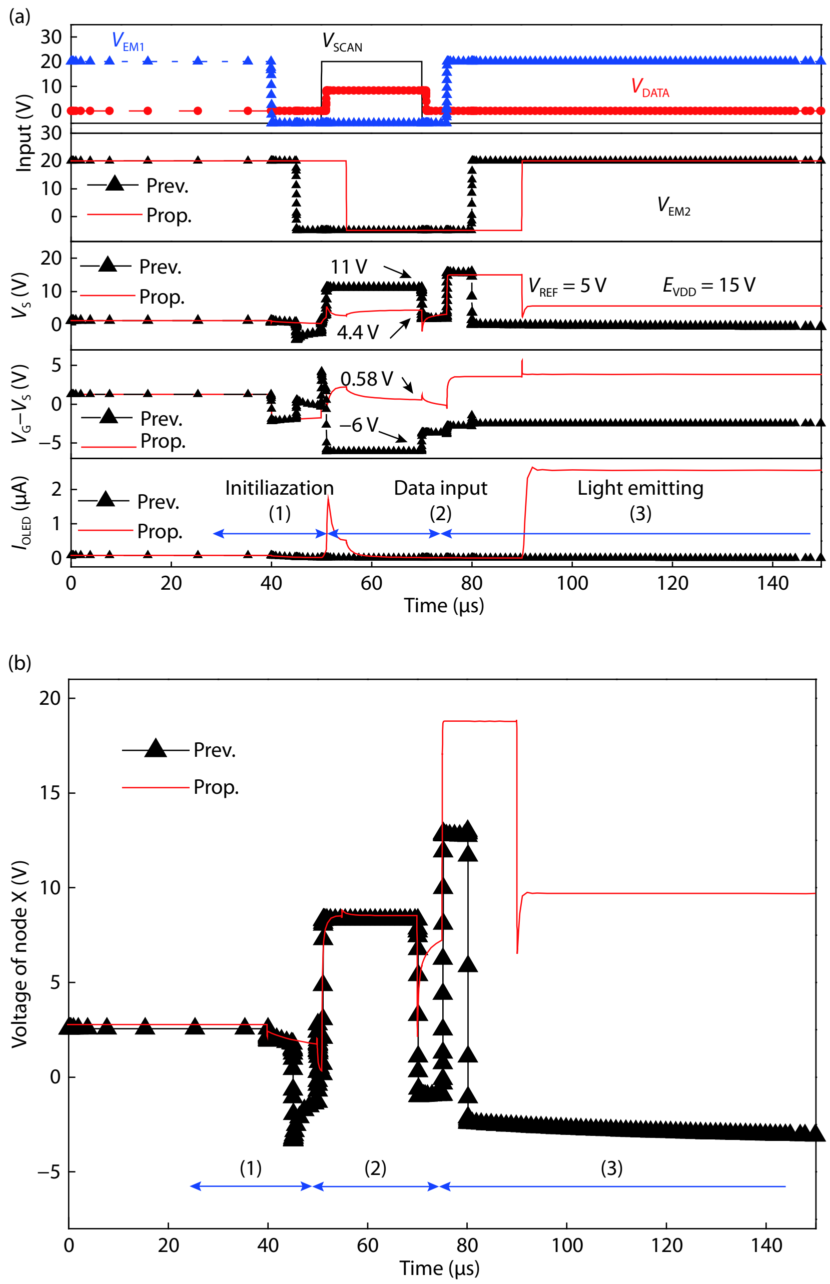

Fig. 4. (Color online) (a) The simulated transent response of V_S, V_{GS}, and I_{OLED} and (b) voltage of node X, with the prvious and the proposed driving method.

most completely transferred to the gate electrode of the driving transistor. According to the charge conservation law, the gate-to-source voltage of T_D can be expressed as $[C_S(V_{DATA} - V_{REF} + V_T) + C_G V_{REF}]/(C_S + C_G)$, Here, C_G is the total capacitance associated with gate electrode of the driving transistor. For practical pixel designs, $C_S \gg C_G$, then the gate-to-source voltage of T_D approximately equals to $(V_{DATA} - V_{REF} + V_T)$, and the conducting current for OLED can be expressed as

$$\begin{aligned} I_{OLED} &= \mu_{FE} C_I \frac{W}{L}(V_G - V_S - V_T)^2 \\ &= \mu_{FE} C_I \frac{W}{L}(V_{DATA} - V_{REF})^2. \end{aligned} \tag{6}$$

Here V_S is the anode voltage of OLED with the turning-on state, which is approximately constant. So the analysis proves that the driving current for OLED of the demonstrated circuit is independent of threshold voltage of the driving transistor.

3.2. Mobility influence on the current error

As previously mentioned, the threshold voltage of the driving transistor is stored on the right terminal of storage capacitance C_S, and the value of the voltage of the source electrode of the driving transistor is dependent on the charging procedure of the driving transistor for the data input period. Then, whether the mobility of IGZO TFT will have an influence on the extracted threshold voltage should be checked through transient analysis. Here, simulation investigations for the pixel circuit are carried out using SmartSpice and the design parameters of the proposed pixel clrcuit are listed in Table 2.

Fig. 4 demonstrates the simulated transient response of V_S, V_{GS}, and I_{OLED} (a), and the voltage of node X(b), with the previous and the proposed driving method. It is shown that, the voltage of node X is almost the same for the previous and the proposed method for the initialization and data input phases,

Table 2. Design parameters of the proposed pixel circuit.

Parameter	Value	Parameter	Value
V_{SCAN} (V)	−5 to 20	$(W/L)_{TS1}$ (μm/μm)	10/10
V_{EM1} (V)	−5 to 20	$(W/L)_{TS2}$ (μm/μm)	10/10
V_{EM2} (V)	−5 to 20	$(W/L)_{TEM1}$ (μm/μm)	10/10
V_{DATA} (V)	5 to 10	$(W/L)_{TEM2}$ (μm/μm)	10/10
E_{VDD} (V)	15	$(W/L)_{TD}$ (μm/μm)	50/10
E_{VSS} (V)	−3	C_S (pF)	0.3
V_{REF} (V)	5	C_{OLED} (pF)	0.5

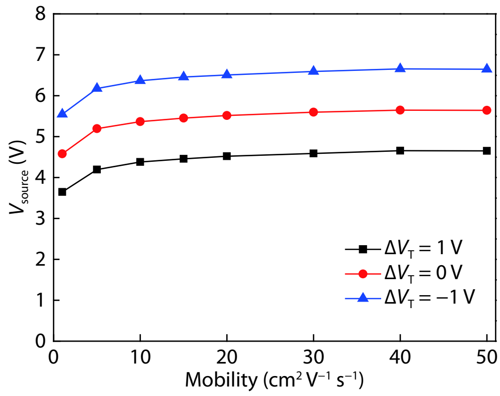

Fig. 5. (Color online) The source voltage of driving transistor with the increase of mobility for different threshold voltage shift.

but there are derivations in the light emitting phase. For the previous timing scheme, due to the lack of proper initialization phase, the voltage of the source electrode of T_D (i.e. V_S) is prone to fluctuate with the input voltage, which results in the failure of programming of V_{GS} and I_{OLED}. These comparison results further prove the previously illustrated analysis.

Fig. 5 shows the voltage of source electrode versus the mobility of IGZO TFT with the threshold voltage shift. Here, the source voltage is extracted at the end of the data input procedure. The mobility varies from 1 to 50 $cm^2V^{-1}s^{-1}$ with the threshold-voltage shift from −1 to 1 V. It is observed that the extracted voltage of source electrode increases with the mobility due to the enhanced charging ability of driving transistor. But once the mobility is higher than 5 $cm^2V^{-1}s^{-1}$, V_S starts to saturate. This is because the loading capacitance at the source electrode of driving transistor is relatively small for the driving transistor. In the demonstrated pixel circuit, the driving transistor is isolated from the capacitance of OLED by the switching transistor T_{EM}, which is controlled by V_{EM2}. Then, for the 'source follower' structure, the loading capacitance of the threshold voltage extraction is relatively small. This is the main improvement of the discussed pixel circuit compared to the previous one[10], which claim that the threshold voltage extraction is strongly dependent on the mobility of IGZO TFT.

Fig. 6 shows the programmed current error with the driving current of 1 μA, for different threshold voltage shift. Here, the current error rate is defined as $[I_{OLED}(\Delta V_T)-I_{OLED}(\Delta V_T = 0)]/I_{OLED}(\Delta V_T = 0)$. It is observed that, for the mobility variation from 1 to 50 $cm^2V^{-1}s^{-1}$, the compensating error is almost constant. The current error seems little large for high resolutions. For example, for a 6-bit resolution, the current error is required to be less than 1.56% (i.e. 2^{-6}).This might be attributed to the large parasitic capacitance of back gate IGZO TFTs. Due to the voltage drop at the parasitic capacitance, the extracted threshold voltage cannot be accurately added to the gate-to-source voltage of the driving transistor as shown in Eq. (6). If new processes are adopted, such as top gate IGZO TFT with self-aligned source/drain, then it is possible that the programmed current error can be substantially decreased. To sum up, the influence of mobility on the current error isn't so direct, and the current error cannot be decreased by merely increasing the mobility of IGZO TFTs.

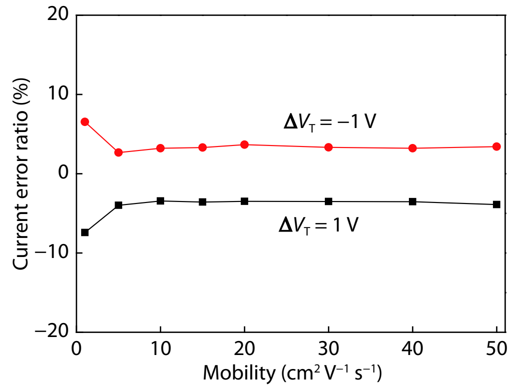

Fig. 6. (Color online) The programmed current error versus mobility for different threshold voltage shift.

3.3. Mobility influence on AMOLED layout

It is expected that, with higher effective mobility, the dimension of the TFT can be decreased. For the four switching transistors, i.e. T_{S0}, T_{S1}, T_{EM1} and T_{EM2}, the dimensions are chosen to be the smallest, thus further increase of mobility is of no use. But for the driving transistor, the channel width can indeed be decreased, if increased mobility TFTs are used as shown in Eq. (6). Furthermore, the capacitance associated with the gate electrode of the driving transistor is decreased. According to the discussions in Section 2, the storing capacitance C_S is determined by

$$C_S = kC_I W_{TD} L_{TD}, \tag{7}$$

where k is an empirical parameter. With the increase of k, the voltage loss due to the parasitic and the gate-to-channel capacitance can be neglected. Further, as IGZO TFTs own the merit of low-leakage current, the decreasing of C_S is possible. In consequence, higher mobility benefits the decreasing of storing capacitance. According to the schematic of Fig. 3, the layout for proposed AMOLED pixel can be derived following the process rules[21]. Comparison results of AMOLED pixel layout with mobility of 10 and 50 $cm^2V^{-1}s^{-1}$ are shown in Fig. 7. The pixel size is decreased from 100 × 100 to 100 × 68 μm^2. In other words, an increase of 32% is obtained in the AMOLED resolution by adopting metal-oxide TFTs with the mobility of 50 $cm^2V^{-1}s^{-1}$.

4. Conclusion

In this paper, the influence of mobility on the performance of AMOLED pixel circuit with IGZO TFTs is investigated. The effective mobility is modeled and parameters for mobility and current-to-voltage characteristics are extracted to fit the measured electric performance of IGZO TFT samples. On the basis of the mobility model, a typical AMOLED pixel, which consists of 5 transistors and 1 capacitor with a new driving timing diagram, is investigated. In additions, the relationship

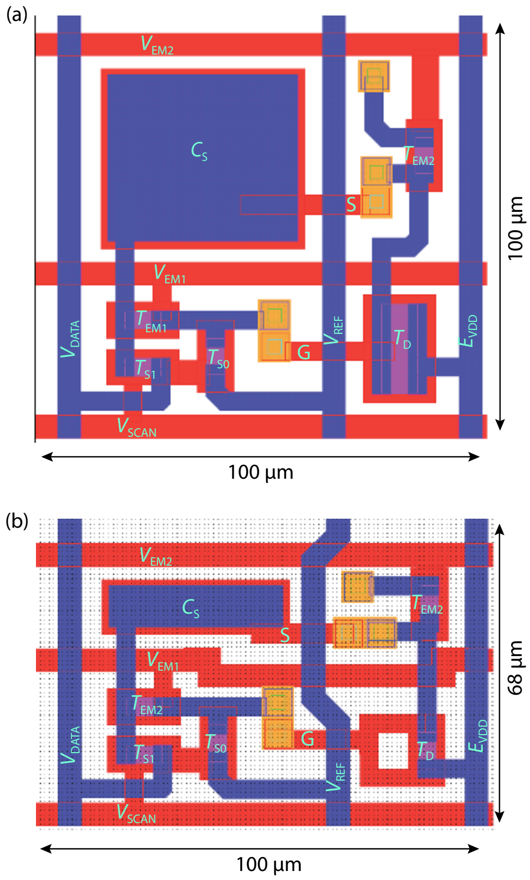

Fig. 7. (Color online) AMOLED pixel layout with mobility of (a) 10 and (b) 50 cm^{2}V^{-1}s^{-1}.

between the pixel circuit performances on the mobility is demonstrated. It is shown that the compensation efficiency of threshold voltage is almost independent on the mobility of IGZO TFTs thanks to the isolation element of the 'source follower' structure and the OLED anode. While the storage capacitance can be decreased with higher mobility, and the pixel resolution is improved as a result. The demonstrated method and results is useful for the design of high performances AMOLED display panel with new metal oxide TFTs.

Acknowledgment

The author would like to thank the anonymous reviewers for their valuable suggestions. This work was supported by National Natural Science Foundation of China (No. 61404002) and the Shenzhen Municipal Scientific Program (No. JCYJ20150626111117384).

References

[1] Mo Y, Kim M, Kang C, et al. Amorphous oxide TFT backplane for large size AMOLED TVs. SID 2010 Digest, 2010: 1037.
[2] Leng C, Wang C, Wang L, et al. Separate frame compensated current-biased voltage-programmed active matrix organic light-emitting diode pixel. IEEE Electron Device Lett, 2014, 35(8), 847
[3] Kawashima S, Inoue S, Shiokawa M, et al. 13.3-in. 8K × 4K 664-ppi OLED display using CAAC-OS FETs. SID 2014 Digest, 2014: 627
[4] Guo X, Silva S. Investigation on the current nonuniformity in current-mode TFT active-matrix display pixel circuitry. IEEE Trans Electron Devices, 2005, 52(11), 2379
[5] Guo X, Silva S. A simple and effective approach to improve the output linearity of switched-current AMOLED pixel circuitry. IEEE Electron Device Lett, 2007, 28(10), 887
[6] Wang M, Wong M. An effective channel mobility-based analytical on-current model for polycrystalline silicon thin-film transistors. IEEE Trans Electron Devices, 2007, 54(4), 869
[7] Nathan A, Kumar A, Sakariya K, et al. Amorphous silicon thin film transistor circuit integration for organic LED displays on glass and plastic. IEEE J Solid-State Circuits, 2004, 39(9), 1477
[8] Nathan A, Lee S, Jeon S, et al. Amorphous oxide semiconductor TFTs for displays and imaging. IEEE J Display Technol, 2014, 10(11), 917
[9] He X, Wang L, Xiao X, et al. Implementation of fully self-aligned homojunction double-gate a-IGZO TFTs. IEEE Electron Device Lett, 2014, 35(9), 927
[10] Kim Y, Kang H, Kim G, et al. Improvement in device performance of vertical thin-film transistors using atomic layer deposited IGZO channel and polyimide spacer. IEEE Electron Device Lett, 2017, 38(10), 1387
[11] Tian Y, Han D, Zhang S, et al. High-performance dual-layer channel indium gallium zinc oxide thin-film transistors fabricated in different oxygen contents at low temperature. Jpn J Appl Phys, 2014, 53, 04EF07
[12] Kumar A, Nathan A, Jabbour G. Does TFT mobility impact pixel size in AMOLED backplanes. IEEE Trans Electron Devices, 2005, 52(11), 2386
[13] Jang Y, Kim D, Choi W, et al. Internal compensation type OLED display using high mobility oxide TFT. SID 2017 Digest, 2017: 76
[14] Estrada M, Cerdeira A, Ortiz-Conde A, et al. Extraction method for polycrystalline TFT above and below threshold model parameters. Solid-State Electron, 2002, 46, 2295
[15] Servati P, Striakhilev D, Nathan A. Above-threshold parameter extraction and modeling for amorphous silicon thin-film transistors. IEEE Trans Electron Devices, 2003, 50(11), 2227
[16] Ryu K, Kymissis I, Bulovic V, et al. Direct extraction of mobility in pentacene OFETs using *C*–*V* and *I*–*V* measurements. IEEE Electron Device Lett, 2005, 26(10), 716
[17] Estrada M, Cerdeira A, Puigdollers J, et al. Accurate modeling and parameter extraction method for organic TFTs. Solid-State Electron, 2005, 49, 1009
[18] Yang M F. Amorphous silicon thin film transistor models and pixel circuits for AMOLED displays. PhD Thesis, University of Waterloo, 2014
[19] Holly Claudia Slade. Device and material characterization and analytic modeling of amorphous silicon thin film transistors. PhD Thesis, University of Virginia, 1997
[20] SMART SPICE User's manual, SILVACO Inc. 2014
[21] Aerts W, Verlaak S, Heremans P. Design of an organic pixel addressing circuit for an active-matrix OLED display. IEEE Trans Electron Devices, 2002, 49(12), 2124